Tubular Hydrogen-Bonded Networks Sustained by Water Molecules

Héctor Carrasco,[†] Concepción Foces-Foces,*[,‡] Cirilo Pérez,*[,§] Matías L. Rodríguez,[§] and Julio D. Martín*[,†]

Contribution from the Departamento de Bioorgánica, Instituto de Investigaciones Químicas, CSIC, Américo Vespucio, s/n, Isla de la Cartuja, 41092 Seville, Spain, Departamento de Cristalografía, Instituto de Química-Física Rocasolano, CSIC, Serrano 119, E-28006 Madrid, Spain, and Instituto de Bioorgánica, Universidad de La Laguna, CSIC, Ctra. Vieja de la Esperanza, 2, 38206 La Laguna, Tenerife, Spain

Received April 23, 2001

Abstract: The design concept of functional solids relies on controlling the topology of crystal packing through exploitation of weak intermolecular forces. In the context of cyclic aggregates, the ability to anticipate the consequences of ring constituents and their stereochemistries on ring conformation is vitally important since even an apparently slight structural change effected on molecules can dramatically alter the crystal structure. We have found that solid-state structures formed by hydroxy acids with a general structure (±)-**1** depend on steric interactions. Thus, with the exception of molecules **1b** and **1e,** compounds (±)-**1a**−(±)-**1m**, which possess bulky and conformationally rigid substituents, aggregate by forming tapes and sheets by alternating (+) and (−) subunits held together through carboxylic acid-to-alcohol hydrogen bonds. Homologue (±)-**1n**, with conformationally flexible substituents which allow conformational deformation, gives, by incorporation of molecules of water, an efficient hexagonal assembly which extends to the third dimension to form tubular H-bonding networks. Each puckered channel can be described as interconnected closely packed hexagons in chairlike conformations. The ethyl groups presented in (±)-**1n** gave the volume required to lock the inner hexagonal wall into a rigid structure. Attempts to obtain cyclic aggregates using small substituents, compounds (±)-**1o**−(±)-**1q**, failed. The observed supramolecular assemblies of the anhydrous compounds can be classified into one-dimensional strands and two-dimensional sheets, while three-dimensional networks are present only in the hydrated molecules (**1b**, **1e**, and **1n**). The crystal structure of the anhydrous (±)-**1n** compound confirms the important role played by water molecules in the formation of tubular structures.

Introduction

Planning the synthesis of molecular materials is commonly frustrated by the absence of reliable structural functions required for the systematic design of crystal lattices with a predictable structure. However, when molecules associate, they recognize motifs containing patterns of interactions.[1] These types of interactions are now beginning to be rationalized, having been characterized as "modules",[2] "supramolecular synthons"[3] in crystal engineering, or "synkinons"[4] in biological assemblies. Such "synthons" are structural units that can be assembled by intermolecular interaction and perform the same focusing role that conventional synthons[5] play in molecular synthesis. Thus, noncovalent assemblies and their structural features can be rationalized following the complementary algorithms that define target[6] and diversity[7] oriented synthesis. Planning the synthesis from a defined starting product (P) to provide collections of small molecules to gain access to a structurally complex target (T) comprises a unique P/T relation similar to the evolutionary principles underlying the election of biosynthetic pathways. This methodology requires the synthesis of individual analogues in order to select the one that organizes according to a predefined architecture. This concept is similar to the way in which, for example, the structures of small molecules are modified in order to optimize their ability to bind a preselected protein target.

The hydroxy acid (±)-**1n**[8] incorporates one molecule of water to form, in the crystalline state, a hexagonal macrocycle [(+)-**1n**·H_2O·(−)-**1n**·H_2O]$_3$, which self-assembles to give a hollow tubular structure {[(+)-**1n**·H_2O·(−)-**1n**·H_2O]$_3$}$_n$. This was the first example of a structurally characterized non-natural molecular aggregate with optimized information to deliver a defined mode of assembly. Furthermore, the energetics of the close packing[9] were maximized by both the effectiveness of the H-bond pattern and the chairlike conformation of the hexagonal macrocycle,[10] such that self-organization could take place in polar or nonpolar solvents from which crystals of (±)-**1n** grew.

* Authors for correspondence.
† Instituto de Investigaciones Químicas, Seville.
‡ Instituto de Química-Física, Madrid.
§ Instituto de Bioorgánica, La Laguna, Tenerife.

(1) (a) Schmidt, G. M. J. *Pure Appl. Chem.* **1971**, *27*, 647. (b) Desiraju, G. R. *Crystal Engineering: The Design of Organic Solids*; Elsevier: New York, 1989. (c) Jorgensen, W. L. *Science* **1991**, *254*, 954. (d) For a recent review, see: Zaworotko, M. J. *Chem. Commun.* **2001**, 1.

(2) Russell, V. A.; Ward, M. D. *Chem. Mater.* **1996**, *8*, 1654.

(3) (a) Desiraju, G. R. *Angew. Chem., Int. Ed. Engl.* **1995**, *34*, 2311. (b) Nangia, A.; Desiraju, G. R. *Supramolecular Synthons and Pattern Recognition* in *Topic Current Chemistry*; Springer-Verlag: Berlín, 1998; Vol. 198, p 58.

(4) Fuhrhop, J.-H.; Rosengarten, B. *Synlett* **1997**, 1015.

(5) Corey, E. J. *Pure Appl. Chem.* **1967**, *14*, 19.

(6) (a) Corey, E. J.; Cheng, X.-M. *The Logic of Chemical Synthesis*; Wiley: New York, 1989. (b) Nicolaou, K. C.; Sorense, E. J. *Classics in Total Synthesis: Targets, Strategies, Methods*; VCH: Weinheim, 1996.

(7) Schreiber, S. L. *Science* **2000**, *287*, 1964.

(8) Preliminary report plus background discussion: Pérez, C.; Espínola, C. G.; Foces-Foces, C.; Núñez-Coello, P.; Carrasco, H.; Martín, J. D. *Org. Lett.* **2000**, *2*, 1185.

(9) Close packing has long been recognized as a primary determinant of molecular crystal structures. Kitiagorodskii, A. I. *Organic Chemical Crystallography*; Consultants Bureau: New York, 1961.

10.1021/ja011028t CCC: $20.00
Published on Web 11/06/2001

Chart 1

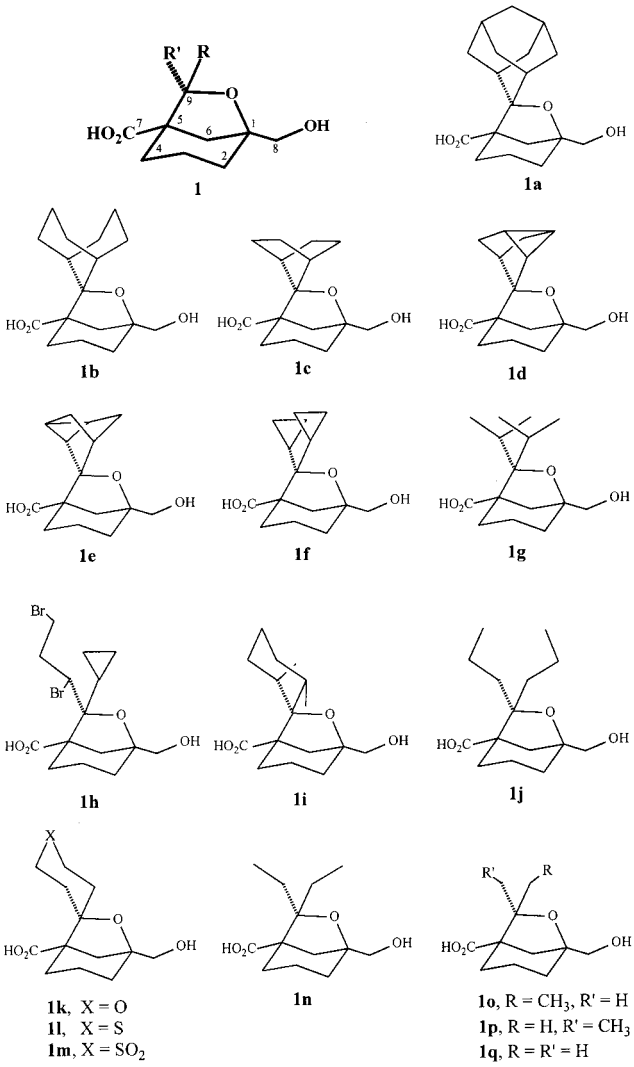

In this paper, compounds of general structure (±)-**1** (Chart 1) are presented that were synthesized with the sole purpose of selecting the one that specifically gave a tubular structure in solid state. Although a systematic effort has been made to identify polymorphs, they have not been observed for any of the compounds studied.

One of the problems associated with incorporating organic molecules in the design of porous solids is the complexity and lack of directionality of intermolecular forces.[11] In the absence of suitable guest molecules occupying framework voids, this isotropy generally leads to denser structures due to closer packing.[12] More directional hydrogen-bonding networks have been selectively used to direct the self-assembly of suitably encoded component molecules to control the size and shape of cavities.[13] However, these networks normally tend to self-interpenetrate, filling the voids left in the initial organization. Generally, the end result is a dense structure. Considerable effort in this area has focused on discrete H-bonded cyclic assemblies containing between 3 and 10 molecules.[13,14] Depending on the nature of the cyclic aggregates, even the closest packing motifs of such building blocks could exhibit significant porosity, with the added advantage that the closest packing would prevent interpenetration.

Scheme 1. Schematic Representation of How the Translational Symmetry of Individual Molecules and Thus Their Packing Form Reversibly, with Nucleation and Growth of Crystal Depending on the Linear (A) versus Cyclic (B) Aggregation

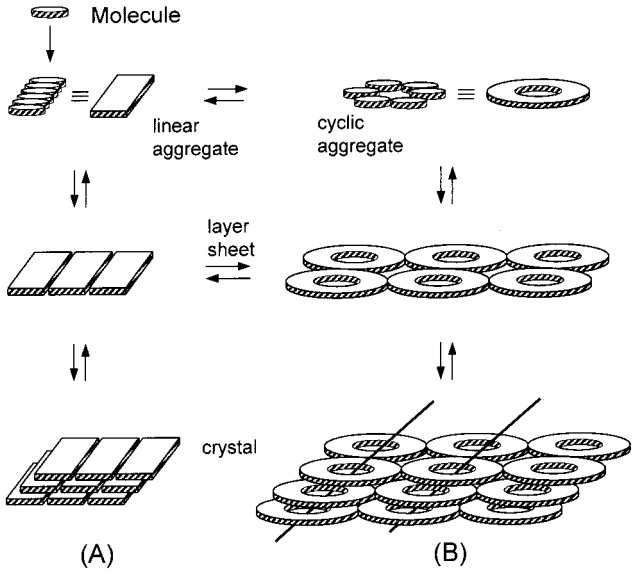

Since H-bonded organic structures form reversibly and exhibit slow kinetics for nucleation and crystal growth,[15] both linear and cyclic states of aggregation should coexist in equilibrium (Scheme 1). Thus, extended chain or cyclic structures can be expected to be selectively obtained by carefully controlling the steric factors that lead to the closest packing of the components.[16] In our strategy, this linear-to-cyclic equilibrium includes an intimate combination of the racemic molecules with molecules of water (i.e., (±)-**1n** ⇄ (±)-**1n**·H_2O), where each water

(10) Cyclic assemblies are formed because they are energetically favored over polymeric ones, not because H-bonding specifically guides the formation of cyclic aggregates. (a) Lady, J. H.; Whetsel, K. B. *J. Phys. Chem.* **1964**, *68*, 1001. (b) For a recent review, see: Sherrington, D. C.; Taskinin, K. A. *Chem. Soc. Rev.* **2001**, *30*, 83.

(11) (a) Gavezzotti, A. *Acc. Chem. Res.* **1994**, *27*, 309. (b) Russell, V. A.; Evans, C. C.; Li, W.; Ward, M. D. *Science* **1997**, *276*, 575.

(12) Bishop, R. *Chem. Soc. Rev.* **1996**, 311.

(13) For reviews, see: (a) Whitesides, G. M.; Simanek, E. E.; Mathias, J. P.; Seto, C. T.; Chin, D. N.; Mammen, M.; Gordon, D. M. *Acc. Chem. Res.* **1995**, *28*, 37. (b) Conn, M. M.; Rebek, J., Jr. *Chem. Rev.* **1997**, *97*, 1647. (c) Lawrence, D. S.; Jiang, T.; Levett, M. *Chem. Rev.* **1995**, *95*, 2229. (d) Philp, D.; Stoddart, J. F. *Angew. Chem., Int. Ed. Engl.* **1996**, *35*, 1154. (e) Melendez, R. E.; Hamilton A. D. *Topics in Current Chemistry*; Springer-Verlag: Berlin, 1998; Vol. 198. (f) Chin, D. N.; Zerkowski, J. A.; MacDonald, J. C.; Whitesides, G. M. In *Strategies for the Design and Assembly of Hydrogen Bonded Aggregates in the Solid State*; Whitesell, J. T., Ed.; John Wiley & Sons: London, 1998; p 185.

(14) For recent examples, see: (a) Marsh, A.; Silvestry, M.; Lehn, J.-M. *Chem. Commun.* **1996**, 1527. (b) Mascal, M.; Hext, N. M.; Warmuth, R.; Moore, M. H.; Turkenburg, J. P. *Angew. Chem., Int. Ed. Engl.* **1996**, *35*, 2204. (c) Kolotuchin, S. V.; Zimmerman, S. C. *J. Am. Chem. Soc.* **1998**, *120*, 9091. (d) Vreekamp, R. H.; Duynhoven, J. P. M.; Hubert, M.; Verboom, W.; Reinhoudt, D. N. *Angew. Chem., Int. Ed. Engl.* **1996**, *35*, 1215. (e) Zimmerman, S. C.; Zeng, F.; Reichert, D. E. C.; Kolotuchin, S. V. *Science* **1996**, *271*, 1095. (f) Zimmerman, S. C.; Duerr, B. F. *J. Org. Chem.* **1992**, *57*, 2215. (g) Boucher, E.; Simard, M.; Wuest, J. D. *J. Org. Chem.* **1995**, *60*, 1408. (h) Yang, J.; Fan, E.; Geib, S. J.; Hamilton, A. D. *J. Am. Chem. Soc.* **1993**, *115*, 5314. (i) Forman, S. L.; Fettinger, J. C.; Piaraccini, S.; Gotarelli, G.; Davies, J. T. *J. Am. Chem. Soc.* **2000**, *122*, 4060. (j) Plant, D. J.; Lund, K. M.; Ward, M. D. *Chem. Commun.* **2000**, 769. (k) Mascal, M.; Hext, N. M.; Warmuth, R.; Arnall-Culliford, J. R.; Moore, M. H.; Turkenburg, J. P. *J. Org. Chem.* **1999**, *64*, 8479. (l) Fenniri, H.; Mathivanan, P.; Vidale, K. L.; Sherman, D. M.; Hallenga, K.; Wood, K. V.; Stowell, J. G. *J. Am. Chem. Soc.* **2001**, *123*, 3854.

(15) For recent studies related to the nucleation rates as function of molecular structural parameters, see: (a) ten Wolde, P. R.; Frenkel, D. *Science* **1997**, *277*, 1975. (b) Talenquer, V.; Oxtoby, D. W. *J. Chem. Phys.* **1998**, *109*, 223. (c) Oxtoby, D. W. *Acc. Chem. Res.* **1998**, *31*, 91. (d) Lee, W. T.; Salje, E. K. H.; Dove, M. T. *J. Phys.: Condens. Matter.* **1999**, *11*, 7385. (e) Yan, S.-T.; Vekilov, P. G. *J. Am. Chem. Soc.* **2001**, *123*, 108.

molecule is involved in three hydrogen bonds (two donors and one acceptor).

Synthetic Rationale

Ring-closing reactions leading to covalently bonded six-membered rings proceed highly effectively as a result of low-energy conformations that place the reacting termini in close proximity and with orientations suitable for bond formation. Similarly, in noncovalently bonded assemblies, favorable conformations along with entropic factors which favor rings over linear polymeric structures would give highly effective cyclic organizations. In the solid state, maintaining this idealized low-energy conformation must be based upon a combination of chemical and crystallographic principles.[17] The most important chemical concept is that of the complementarity of the H-bond functionality set, a combination of atoms with hydrogen bond donors and acceptors matched in terms of number, shape, and interatomic distances. The important crystallographic concept is an accounting of the symmetry operator that interrelates the two molecules of each intermolecular hydrogen bond. For any supramolecular structure, molecules must be chosen with the proper size and shape to achieve the closest molecular packing.[18] One illustration of the strategy followed using a hypothetical model molecule is depicted in Scheme 2. Because in axially oriented hydroxyl/carboxylic acid functions the "like-to-unlike" carboxylic acid-to-alcohol H-bonds is the somewhat more favorable pattern in terms of energy,[19] the dimeric H-bonding network (**IV**) was anticipated to be the most likely possibility. Our strategy was to construct robust H-bonded arrays by using molecular descriptors with an unbalanced H-bond donor/acceptor ratio[20] (−OH, −O−, $-CO_2H$; d/a = 0.5) and then promote reversion to cyclic aggregate (**I**) by readdressing the d/a imbalance by inclusion of molecules of water (−OH, −O−, H_2O, $-CO_2H$; d/a = 0.8). The reasoning behind this approach is that the incorporation of molecules of water in hydrophilic H-bonding networks might disrupt the dimeric motif, creating a single-strand array (**II**) in a favorable conformation for ring packing. Furthermore, the three-fold symmetry of the chairlike hexameric aggregate (**I**) results in an extension of the H-bonded lattice in a direction perpendicular to the plane of the ring. It was expected that these hexamers might form atop one another by H-bonding in such a fashion that extended channel structures would be generated.

In compounds of general structure **1** and because of the free rotation around the C_1-C_8 bond, the cyclic H-bonding synthon

Scheme 2. "Retrosynthetic Analysis" of Design for Cyclic Hexameric Aggregate (**I**) of the Hypothetical Model A by Addition of Molecules of Water to an Axial Oriented Carboxylic Acid/Alcohol Ladder-type Network (**IV**)[a]

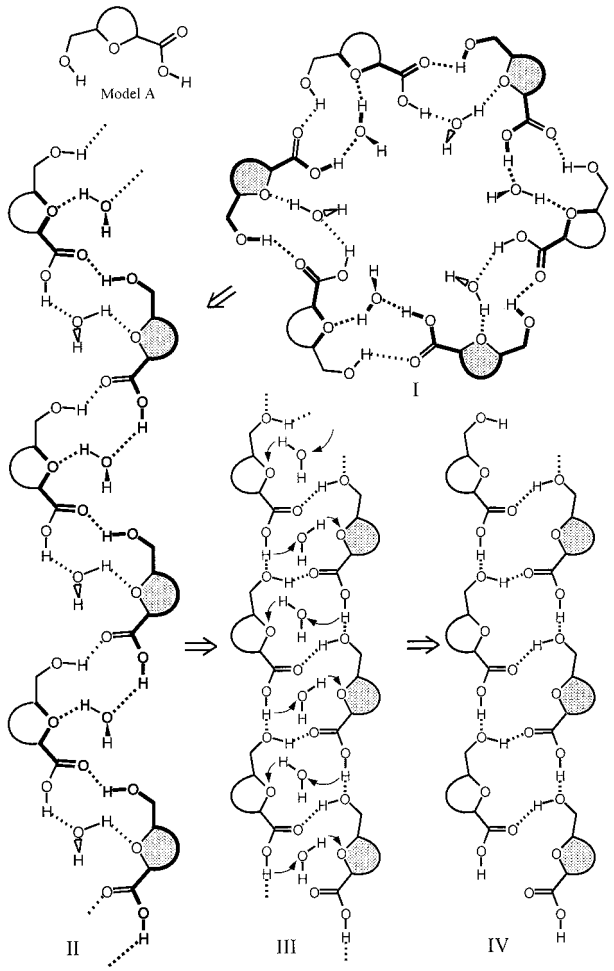

[a] Enantiomers are distinguished by shading, and hydrogen bonds are indicated by dotted lines.

due to the exclusive participation of complementary carboxylic acid/primary alcohol functionalities should provide highly ordered one- or two-dimensional networks. Because the H-bond pattern is centrosymmetric, an ambiguity arises in the expression of information, leading to tape and sheet aggregates (Scheme 3). Thus, depending upon the conformation of the $O-C_1-C_8-O$ torsion angle, an anti conformation should give a 1-D assembly (tape), while a gauche conformation should extend the H-bonding pattern in 1-D (tape) or 2-D (sheet) assemblies. Furthermore, this cyclic H-bond network should form wavy layer structures, which organize in a parallel (A) or antiparallel (B, C) manner without any void space in the lipophilic sites. Consequently, these arguments can be used as a platform with which to control and predict molecular packing for hydrated structures. Thus, the parallel organization (A, A′) sets a zigzag structuring of monomers equilibrated by anti/gauche conformational exchange of the torsion angle formed by $HO-C_1-C_8-O$ bonds. This equilibrium, which is limited by steric interactions between appendages of the monomers, will lead, by hydration with participation of the ether oxygen, to single-stranded chains formed "head-to-tail" with alternating distribution of enantiomers (**IV** ⇄ **II**, Scheme 2). Since the centrosymmetric chairlike hexagonal ring structure (**I**) requires the chirality at adjacent vertexes to be opposite, the **II**-to-**I** equilibrium can be reached by hydration of double strands on the gauche conformations

(16) (a) Zerkowski, J. A.; Seto, C. T.; Wierda, D. A.; Whitesides, G. M. *J. Am. Chem. Soc.* **1990**, *112*, 9025. (b) Lehn, J.-M.; Mascal, M.; De Cian, A.; Fischer, J. *J. Chem. Soc., Chem. Commun.* **1990**, 479. (c) Whitesides, G. M.; Mathias, J.-P.; Seto, C. T. *Science* **1991**, *254*, 1312. (d) Zerkowski, J. A.; Seto, C. T.; Whitesides, G. M. *J. Am. Chem. Soc.* **1992**, *114*, 5473. (e) Lehn, J.-M.; Mascal, M.; De Cian, A.; Fischer, J. *J. Chem. Soc., Perkin Trans. 2* **1992**, 461. (f) Zerkowski, J. A.; MacDonald, J. C.; Seto, C. T.; Wierda, D. A.; Whitesides, G. M. *J. Am. Chem. Soc.* **1994**, *116*, 2382. (g) Zerkowski, J. A.; Whitesides, G. M. *J. Am. Chem. Soc.* **1994**, *116*, 4298. (h) Zerkowski, J. A.; Mathias, J.-P.; Whitesides, G. M. *J. Am. Chem. Soc.* **1994**, *116*, 4305. (i) Mathias, J.-P.; Simanek, E. E.; Zerkowski, J. A.; Seto, C. T.; Whitesides, G. M. *J. Am. Chem. Soc.* **1994**, *116*, 4316.

(17) Chang, Y.-L.; West, M.-A.; Fowler, F. W.; Lauher, J. W. *J. Am. Chem. Soc.* **1993**, *115*, 5991.

(18) Chin, D. N.; Palmore, G. T.; Whitesides, G. M. *J. Am. Chem. Soc.* **1999**, *121*, 2215.

(19) As representative examples, see: Miyata, M.; Sada K. In *Comprehensive Supramolecular Chemistry*; MacNicol, D. D., Toda, F., Bishop, R., Eds.; Elsevier Science Inc.: Amsterdam, 1996; Vol. 6, p 147.

(20) When the numbers of potential hydrogen bond donors and acceptors in a crystal are not equal, water, which can donate two and accept one or two hydrogen bonds, can help settle the balance of donors and acceptors. (a) Desiraju, G. R. *Chem. Commun.* **1990**, 426. (b) Etter, M. C. *Acc. Chem. Res.* **1990**, *23*, 120.

Scheme 3. Schematic Construction of Parallel (A, A′) and Antiparallel (B, B′) Assemblies (Tapes) Occurring by Trans (A, B) or Gauche (A′, B′) Conformations of the Torsion Angle Formed by HO−C_8−C_1−O in (±)-**1**[a]

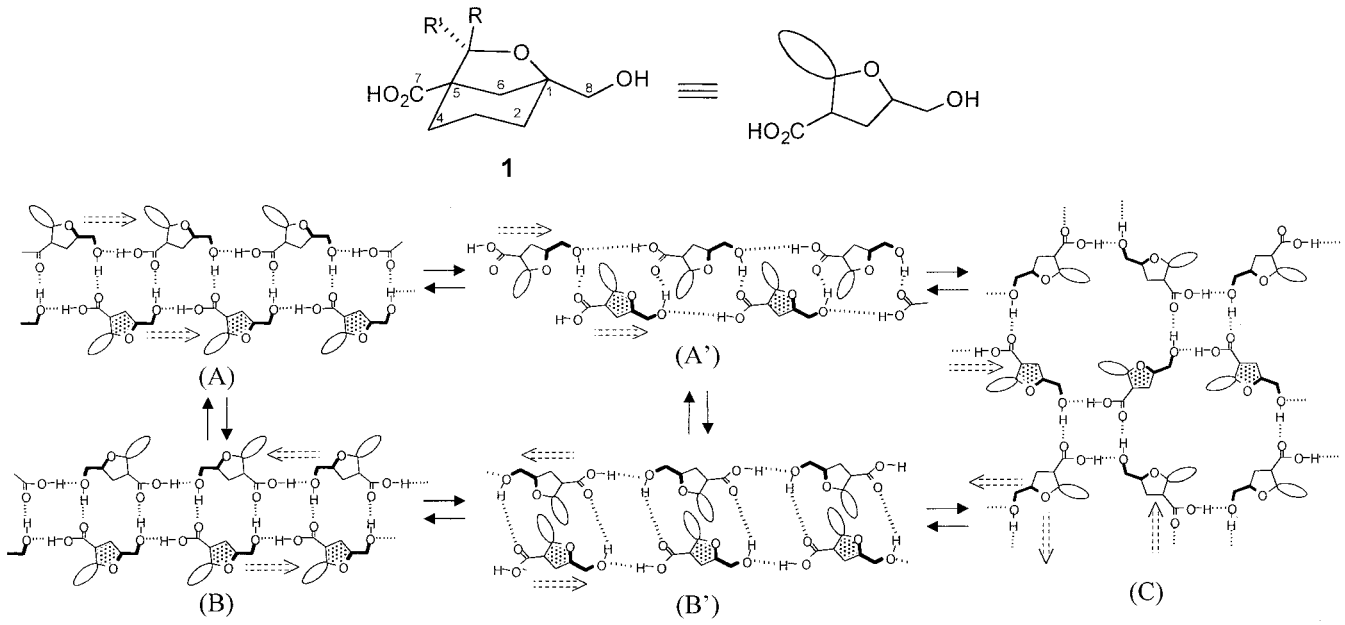

[a] Two-dimensional (sheet) assembly (C) formed by gauche conformation of the above-defined torsion angle. Dashed lines represent hydrogen bonds. Enantiomers are distinguished by shading.

shown by A′ (Scheme 3). Similar hydration of antiparallel double strands (B, B′) should allow single-stranded "head-to-tail" chains of molecules formed by one of the two enantiomers.

Results

To verify the above predictions, we synthesized a wide range of homologues by changing the number and nature of selected atoms in the general structure (±)-**1** and studied their structural influence in the solid state (Chart 1). Several of these compounds were considered promising candidates to give hollow tubular structures, whereas other molecules were chosen to probe the structural requirements in detail. It is also reasonable to assume that the enthalpic contribution toward the formation of a polymer chain and sheet versus ring structures will be approximately equal, and therefore the products of these equilibria will be primarily determined by entropic contributions to the free energy.[10]

Racemic compounds **1a**−**f** and **1i**−**q** were synthesized by condensing the dilithium salt of 3-methylenecyclohexanecarboxylic acid with the appropriate ketone following the synthetic sequence outlined in Scheme 4. Compounds **1g** and **1h** were preparated from **1f** by hydrogenation (H_2/PtO_2) and bromination (Br_2, $CHCl_3$), respectively.

X-ray Crystallography

In the present paper, the structures of compounds (±)-**1a**−(±)-**1d**, **1e**, (±)-**1f**−(±)-**1i**, and (±)-**1k**−(±)-**1p** (no suitable crystals for (±)-**1j**) were obtained) have been determined. The crystal structure of (±)-**1j**·H_2O could not be determined due to difficulties in obtaining suitable single crystals. Several crystallization attempts to obtain both hydrates and anhydrous compounds afforded only compound (±)-**1n** as both anhydrous and monohydrate compounds, whereas (±)-**1b** appears only as a hemihydrate and **1e** as a monohydrate. Selected geometrical parameters for each structure, including those of (±)-**1n**·H_2O[8] and (±)-**1q**,[21] previously reported, are given in Tables 1 and 2 according to the numbering scheme displayed in Figure 1, where the molecular structures of all compounds are shown. For comparison purposes, in all compounds, the same enantiomer has been considered in the asymmetric unit, that is, the one showing a negative value for the C1−C2−C3−C4 torsion angle. However, when two independent molecules are present in the asymmetric unit, the chirality of the second one has been chosen as the one joined to the reference one by hydrogen bonds.

Scheme 4[a]

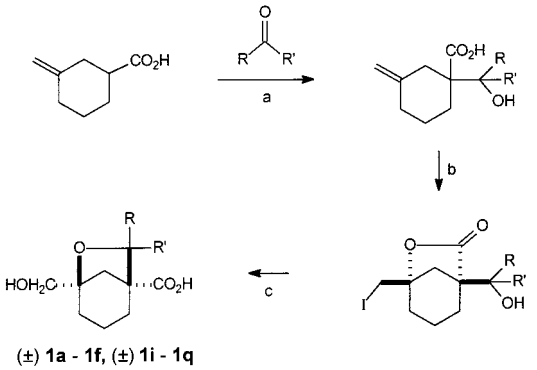

[a] Conditions: (a) DIPA, *n*-BuLi, THF; (b) DIPA, I_2, CH_2Cl_2; (c) THF, KOH aqueous, THF.

The bicyclic core is rather rigid, and the main differences in the common part seem to be a consequence of orientation of the hydroxyl and carboxylic groups with respect to the bicyclic. The most noticeable variation in the bond pattern concerns the C−O lengths and C−C−O angles in the carboxylic group. Both C7−O distances tend to be quite alike, suggesting proton disorder (two sites with half-occupancy factors for the H of the hydroxyl and carboxylic atoms), as is often found in carboxylic derivatives,[22] mainly in those forming dimers. A search of the CSD[23] was undertaken to retrieve compounds containing

(21) Ruiz-Pérez, C.; Rodríguez, M. L.; Martín, J. D.; Pérez, C.; Morales, P.; Ravelo, J. L. *Acta Crystallogr*. **1990**, *C46*, 1507.

(22) Leiserowitz, L. *Acta Crystallogr*. **1976**, *B32*, 775.

(23) Allen, F. H.; Davies, J. E.; Galloy, J. J.; Johnson, O.; Kennard, O.; Macrae, C. F.; Mitchell, E. M.; Mitchell, G. F.; Smith, J. M.; Watson, D. G. *J. Chem. Info. Comput. Sci*. **1991**, *31*, 187.

Table 1. Selected Torsion Angles (deg)

compound	τ1 O1−1−8−O2H	τ2 1−8−O2−H	τ3 4−5−7−O4H	τ4 4−5−7═O3
(±)-**1a**(Mol. A)	179.7(10)	−68	−37.2(16)	140.9(14)
(±)-**1a**(Mol. B)	−177.9(11)	85	42.0(14)	−136.1(13)
(±)-**1b**·$^1/_2H_2O$ (Mol. A)	174.4(3)	−84	144.8(3)	−32.0(6)
(±)-**1b**·$^1/_2H_2O$ (Mol. B)	−77.1(4)	164	−142.8(3)	35.1(5)
(±)-**1c**(Mol. A)	178.2(10)	−68	−35.3(17)	151.0(15)
(±)-**1c**(Mol. B)	−178.1(10)	89	34.4(17)	−147.4(14)
(±)-**1d**	72.2(2)	−136	−17.5(3)	160.9(2)
1e·H_2O	68.4(7)	−116	−28.1(8)	150.8(7)
(±)-**1f**	−178.1(2)	−60	−46.3(2)	132.4(2)
(±)-**1g**(Mol. A)	−60.3(3)	−80	142.2(3)	−36.2(4)
(±)-**1g**(Mol. B)	60.3(3)	131	133.5(2)	−42.1(4)
(±)-**1h**	173.8(4)	46	162.1(5)	−16.2(6)
(±)-**1i**	−68.3(2)	127	126.3(2)	−49.6(2)
(±)-**1k**	56.2(2)	−63	−59.5(2)	119.9(2)
(±)-**1l**	−172.8(5)	−74	−61.2(6)	116.2(7)
(±)-**1m**	−55.1(2)	107	88.8(2)	−87.9(2)
(±)-**1n**·H_2O	56.2(4)	−92	126.5(4)	−51.6(6)
(±)-**1n**	−177.2(3)	−82	−37.9(5)	140.6(4)
(±)-**1o**	69.8(4)	−126	−55.2(6)	125.0(5)
(±)-**1p**	60.5(2)	−61	−65.6(2)	113.3(2)
(±)-**1q**	62.0(3)	−131	−63.5(3)	117.0(3)

Table 2. Selected Bond Distances (Å) and Angles (deg) in the Carboxylic Group

	C5−C7	C7═O3	C7−O4H	C5−C7−O4H	C5−C7═O3
CSD ordered	1.501(17)	1.226(13)	1.301(19)	114.4(16)	122.4(16)
CSD ordered, average	1.501(17)	1.263(9)	1.263(9)	118.4(4)	118.4(4)
(±)-**1a**(Mol. A)	1.521(19)	1.192(16)	1.326(16)	113.0(13)	123.1(13)
(±)-**1a**(Mol. B)	1.528(18)	1.198(15)	1.297(15)	113.9(12)	124.1(12)
(±)-**1b**.1/2 H_2O(Mol. A)	1.527(5)	1.199(5)	1.341(5)	113.0(3)	124.8(3)
(±)-**1b**.1/2 H_2O(Mol. B)	1.517(5)	1.212(5)	1.323(5)	114.0(3)	124.5(4)
(±)-**1c**(Mol. A)	1.519(19)	1.171(18)	1.347(19)	111.1(16)	124.9(18)
(±)-**1c**(Mol. B)	1.508(19)	1.235(16)	1.294(15)	114.2(14)	122.2(14)
(±)-**1d**	1.519(3)	1.198(3)	1.325(3)	113.2(2)	124.0(2)
1e·H_2O	1.512(9)	1.217(8)	1.318(8)	114.7(7)	123.1(8)
(±)-**1f**	1.521(3)	1.206(3)	1.317(3)	113.4(2)	123.9(2)
(±)-**1g**(Mol. A)	1.539(4)	1.212(4)	1.313(4)	114.9(3)	122.4(3)
(±)-**1g**(Mol. B)	1.564(5)	1.181(4)	1.308(4)	115.6(3)	124.9(3)
(±)-**1h**	1.536(7)	1.241(7)	1.261(7)	116.6(5)	118.1(6)
(±)-**1i**	1.525(3)	1.205(3)	1.319(3)	113.2(2)	124.0(2)
(±)-**1k**	1.508(2)	1.239(2)	1.291(2)	116.5(1)	120.6(1)
(±)-**1l**	1.522(8)	1.200(8)	1.326(7)	113.3(5)	125.1(5)
(±)-**1m**	1.517(2)	1.206(2)	1.324(2)	112.5(1)	124.2(1)
(±)-**1n**·H_2O	1.495(5)	1.202(5)	1.322(5)	114.7(3)	123.7(3)
(±)-**1n**	1.522(5)	1.200(5)	1.311(5)	114.4(4)	123.4(4)
(±)-**1o**	1.500(6)	1.225(6)	1.295(6)	115.5(4)	121.7(4)
(±)-**1p**	1.512(3)	1.241(2)	1.291(2)	116.4(2)	120.7(2)
(±)-**1q**	1.498(4)	1.223(4)	1.319(4)	114.8(3)	124.4(3)

CSD results for dicarboxylic derivatives (96 ordered Csp3-COOH fragments) with R < 0.050. Number in parentheses corresponds to the standard deviation of the sample.

carboxylic acid and to update the geometry of the group given by Leiserowitz.[22] Organic compounds subject to the criterion of $R < 0.050$ to assess the quality of the data (Table 2) were sorted out according to the presence or absence of proton disorder. In (±)-**1h** and (±)-**1k**, C−O distances and O═C−C and HO−C−C angles are close to the average CSD values, and a disorder could be established. In the first case, the disorder also affects the hydroxyl OH group, although the hydrogen bond motif is maintained.

Inspection of the secondary structure (Table 3), due to O−H···O interactions, reveals the following features:

(1) Except in **1e**, both enantiomers are present in the crystal structure.

(2) Only three compounds crystallize as hydrates ((±)-**1b**, (±)-**1n**, and (+)-**1e**).

(3) For the anhydrous cases, two hydrogen bond motifs are found, ribbons and layers.

(4) The common feature of all anhydrous structures (except in (±)-**1k**, **o**, and **p**) is that the hydroxyl in the carboxylic group (O4) always acts as a donor to the other hydroxyl oxygen in a reasonably short hydrogen bond (from 2.578(6) Å in (±)-**1l** to 2.710(5) Å in (±)-**1h**) or to the carbonyl of the carboxylic group, and it never accepts a hydrogen bond except in (±)-**1k**,**p**,**q**, while hydroxyl O2 acts as both a donor and an acceptor.

The supramolecular assemblies can be classified into (a) one-dimensional (ribbons), (b) two-dimensional (sheets), and (c) three-dimensional networks.

(a) One-Dimensional Network. The secondary structure of (±)-**1a**, **c**, **f**, **h**, **k**, **l**, **m**, **n**, and **p** consists of chains of head-to-tail hydrogen-bonded molecules produced by translation, all

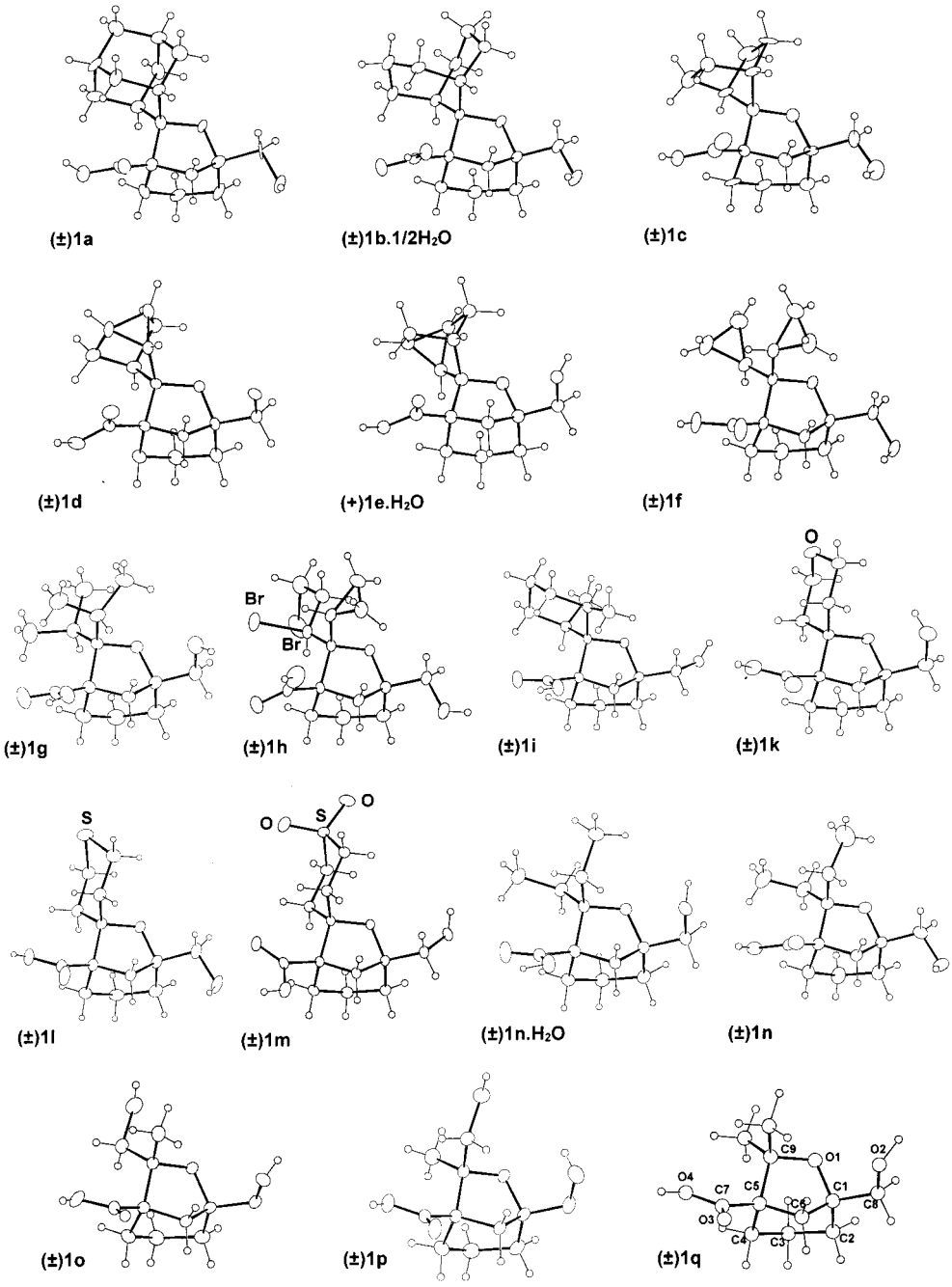

Figure 1. Molecular structures of all compounds showing the numbering scheme. Thermal ellipsoids are drawn at the 30% probability level.

having the qualitative graph set C(8) (graph set analysis[24] implemented in the RPLUTO program[25]). The similarities and discrepancies in this graph set descriptor are evidenced in Figure 2, where the OH···O bonds have been labeled a−c in the order of appearance in Table 3. Two chains of enantiomeric molecules (inversion center: (±)-**1c**,**f**,**h**,**n**,**m**,**o**,**p**, glide plane in (±)**1l**) or two crystallographically independent molecules of both enantiomers ((±)-**1a** and **c**) are linked together, generating rings of different sizes. Furthermore, the acceptor or donor atoms differ from one compound to another, that is, O4H···O2 in (±)-**1a**,**c**,**f**,**l**,**m**,**n**, O2H···O3 in (±)-**1h**, and O2H···O4 in (±)-**1k** and (±)-**1p**.

The ribbon in (±)-**1m** is closely related to those in (±)-**1f** and **h**, where the differences in the size of the rings can be assigned to the substitution of the O3 acceptor by one of O═S group. In (±)-**1k** and **p**, the common[22] hydrogen bond pattern, $R_2^2(8)$, around inversion centers is observed (Figure 2b). The hydroxyl O2 is involved in a bifurcated hydrogen bond to the ether O1 and the carboxylic group, the last one resulting in a rather long contact [26] (Table 3) that is responsible for the formation of chains. The packing arrangement of (±)-**1o** with the second level graph set is C_2^2 (14), similar to that of (±)-**1k** and **p**, where the intramolecular O2H···O1 bond has been replaced by a O2−H···O1 intermolecular bond (Figure 2b and Table 3).

The relationship between molecular and crystal structure, as far as the secondary structure is concerned, may be understood

(24) Bernstein, J.; Davis, R. E.; Shimoni, L.; Chang, N.-L. *Angew. Chem., Int. Ed. Engl.* **1995**, *34*, 1555.

(25) Motherwell, W. D. S.; Shields, G. P.; Allen, F. H. *Acta Crystallogr.* **2000**, *B56*, 466.

(26) Jeffrey, G. A.; Saenger, A. *Hydrogen Bonding in Biological Structures;* Springer-Verlag: Berlin, Heidelberg, New York, 1991.

Table 3. Hydrogen Bond Geometry (Distances, Å; Angles, deg)

	D−H	H···A	D···A	D−H···A		D−H	H···A	D···A	D−H···A
(a) One-Dimensional Network									
(±)-**1a**									
O2A−H···O3B	0.82	2.25	2.829(15)	127	O2B−H···O3A($x,-1+y,z$)	0.82	1.99	2.768(14)	159
O4A−H···O2A($x,1+y,z$)	0.82	1.84	2.607(14)	156	O4B−H···O2B($x,1+y,z$)	0.82	1.82	2.601(13)	158
(±)-**1c**									
O2−H···O3($1-x,2-y,1-z$)	0.82	1.94	2.738(15)	163	O22−H···O23($1-x,1-y,2-z$)	0.82	1.93	2.732(14)	167
O4−H···O22	0.82	1.79	2.601(14)	173	O24−H···O2($x,-1+y,1+z$)	0.82	1.84	2.601(15)	153
(±)-**1f**									
O2−H···O3($1-x,2-y,1-z$)(dimers)	0.82	2.03	2.740(3)	144	O4−H···O2($-1+x,1+y,z$)	0.82	1.82	2.616(2)	162
(±)-**1h**[a]									
O2−H22···O3($x,1+y,z$)	0.85	1.88	2.729(5)	180	O2−H21···O4 ($-x,1-y,1-z$)	0.85	1.86	2.710(5)	180
O4−H···O2($-x,1-y,1-z$)(dimers)	0.85	1.86	2.710(5)	180	O3−H···O2 ($x,-1+y,z$)	0.85	1.88	2.729(5)	180
(±)-**1k**[a]									
O2−H···O4($1+x,y,z$)	0.92(3)	2.64(3)	3.112(2)	113(2)	O3−H3···O4($1-x,-y,-z$)	0.80(8)	1.84(8)	2.640(2)	174(6)
O4−H4···O3($1-x,-y,-z$)(dimers)	0.78(5)	1.87(5)	2.640(2)	172(4)	O2−H···O1	0.92(3)	2.31(3)	2.810(2)	114(2)
(±)-**1l**									
O2−H···O3($x,3/2-y,-1/2+z$)	0.82	1.91	2.715(6)	169	O4−H···O2($x,y,1+z$)	0.82	1.76	2.578(6)	172
(±)-**1m**									
O2−H···O6($1-x,-y,-z$)(dimers)	0.82	2.13	2.913(2)	161	O4−H···O2($x,1+y,z$)	0.82	1.88	2.691(2)	172
(±)-**1n**									
O2−H2···O3($-x,-y,-z$)(dimers)	0.79(5)	1.95(5)	2.733(4)	173(5)	O4−H4···O2($1+x,1+y,z$)	0.93(5)	1.67(5)	2.585(4)	166(4)
(±)-**1o**									
O2−H···O1($-x,-y,1-z$)(dimers)	0.82	2.04	2.844(4)	168	O4−H···O3($-x,1-y,2-z$)(dimers)	0.82	1.83	2.645(5)	175
(±)-**1p**									
O2−H···O4($x,y,1+z$)	0.82	2.64	3.131(3)	120	O2−H···O1	0.82	2.54	2.849(2)	104
O4−H···O3($1-x,1-y,-z$)(dimers)	0.82	1.83	2.647(2)	173					
(b) Two-Dimensional Network									
(±)-**1d**									
O2−H···O1($1-x,-y,1-z$)	0.84(3)	1.95(3)	2.786(2)	172(3)	O4−H···O2($1-x,1/2+y,3/2-z$)	0.86(3)	1.81(3)	2.661(2)	172(3)
(±)-**1g**									
O2A−H···O2B	0.82	2.07	2.765(4)	143	O2B−H···O3A(($3/2-x,y,-1/2+z$)	0.82	1.89	2.683(3)	164
O4A−H···O2A($3/2-x,y,1/2+z$)	0.82	1.84	2.645(3)	168	O4B−H···O1B($3/2-x,y,-1/2+z$)	0.82	2.09	2.875(3)	161
(±)-**1i**									
O2−H···O1($-x,-y,1-z$)(dimers)	0.82	1.98	2.781(2)	165	O4−H···O2($1/2-x,-y,-1/2+z$)	0.82	1.84	2.651(2)	168
(±)-**1q**									
O2−H···O3($x,1/2-y,-1/2+z$)	1.00	1.98	2.781(3)	135	O4−H···O2($-x,-1/2+y\ 1/2-z$)	0.95	1.69	2.624(3)	167
(c) Three-Dimensional Network									
(±)-**1b**·$^1/_2H_2O$									
O2A−H···Ow($x,1+y,z$)	0.82	1.86	2.674(4)	172	O4B−H···O2A	0.82	1.80	2.618(4)	174
O4A−H···O1A($x,1+y,z$)	0.82	1.91	2.717(4)	167	Ow−Ha···O2B($1-x,-1/2+y,1/2-z$)	0.85	2.09	2.823(4)	144
O2B−H···O1B($-x,1/2+y,1/2-z$)	0.82	2.04	2.828(3)	160	Ow−Hb···O3B	0.85	2.08	2.780(4)	140
1e·H_2O									
O2−H···Ow ($1/2+x,1/2-y,1-z$)	0.82	2.06	2.788(7)	149	Ow−Hb···O1	0.95	1.83	2.786(6)	175
Ow−Ha···O2($-1+x,y,z$)	1.01	1.79	2.713(6)	149	O4−H···Ow($1/2-x,-y,1/2+z$)	1.04	1.65	2.649(6)	159
(±)-**1n**·H_2O									
Ow−Hb···O1	0.92(7)	1.83(7)	2.712(4)	159(6)	O2−H···O3($1/3+x-y,-1/3+x,2/3-z$)	0.92(6)	1.81(7)	2.711(6)	166(5)
Ow−Ha.···O2($x,y,z-1$)	0.86(7)	1.89(7)	2.753(5)	172(6)	O4−H···Ow($1/3+y,2/3-x+y,1/3-z$)	1.04(6)	1.52(7)	2.563(5)	177(10)

[a] Disorder of the H atom in the −OH and −COOH groups. (±)-**1h**: pp(H4) = 0.62(6), pp(H3) = 0.38(6). (±)-**1k**: pp(H3) = pp(H4) = 0.50. pp is the occupancy factor.

by examining the orientation of the hydroxyl and carboxylic groups with respect to the bicyclic core (Table 1). In all compounds, the H atom of the carboxylic group is in a synplanar conformation (trans to C5), as pointed out by Leiserowitz[22] as the most probable one for intermolecular contacts. Apart from distortions and due to the planarity of the carboxylic group $\tau 4 \sim 180 + \tau 3$ (module π), the independent variables are $\tau 1$, $\tau 2$, and $\tau 3$.

The combination of these three torsion angles can be summarized at idealized positions as follows. Ribbons can be observed (a) always when the hydroxyl O atom is trans to the ether one, being an acceptor or a donor group depending on the conformation of its H and the carboxylic group (a twist of 180° as mentioned above) or (b) in gauche conformations, +60 or −60° for $\tau 1$ and presenting opposite values for $\tau 2$ and $\tau 3$.

(±)-**1a**,**c**,**f**,**l**,**n**: $\tau 1 \sim 180$, $\tau 2 \sim -60 \pm 30$, and $\tau 3 \sim -30 \pm 30°$

O4H···O2 and O2H···O3 are responsible for the formation of the chain and the linkage between two chains respectively to give ribbons.

(±)-**1h**: $\tau 1 \sim 180$, $\tau 2 \sim 30$, and $\tau 3 \sim 150 \pm 30°$

That means that a twist of 180° in the carboxylic acid and now the O2−H···O3 bond is responsible for the formation of the chains, and the O4H···O2 bond is responsible for the link of two chains.

(±)-**1k** and **p**: $\tau 1 \sim 60$, $\tau 2 \sim -60$, and $\tau 3 \sim -60°$

(±)-**1o**: $\tau 1 \sim 60$, $\tau 2 \sim -60$, and $\tau 3 \sim -120°$

(±)-**1m**: $\tau 1 \sim -60$, $\tau 2 \sim 120$, and $\tau 3 \sim 90°$

Semiempirical AM1 calculations[27] on model (±)-**1q** give evidence that the molecular stability is affected by the disposition of the hydroxyl O2 group ($\tau 1$ = O1−C1−C8−O2). The gauche conformations ($\tau = -60$ or 60°) are almost isoenergetic

(27) AMPAC Version 5.0., Semichem Inc., Shawnee, KS 66216.

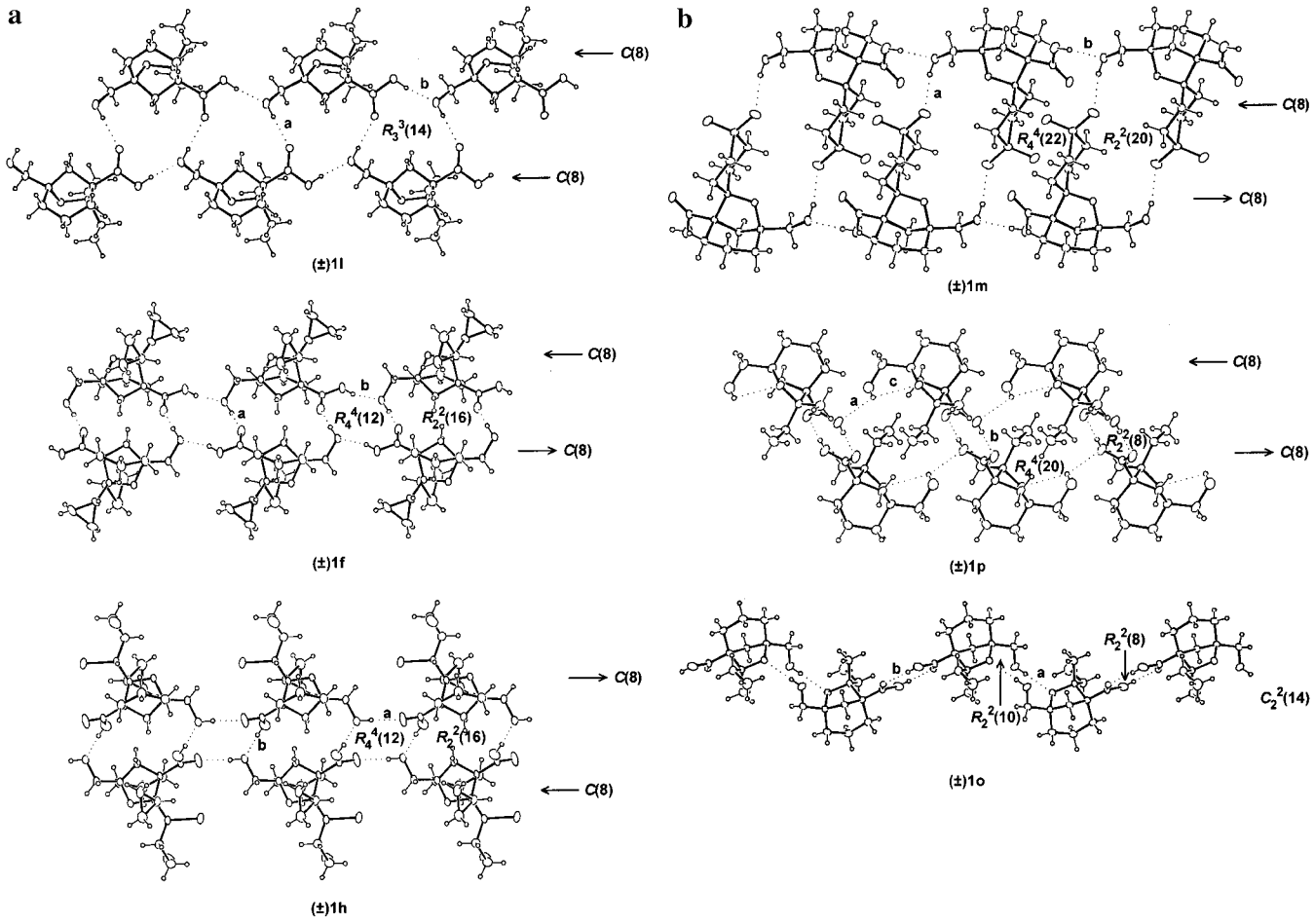

Figure 2. Secondary structures of compounds (±)-**1l**, **f**, **h**, **m**, **p**, and **o** illustrating the different types of 1-D hydrogen-bonding pattern (ribbons). The results of the basic first- and second-level graph-set analysis have been included involving the O—H···O hydrogen interactions (dotted lines) labeled a−c in the order of appearance in Table 3. The arrows close to the C(8) notation represent the parallel or antiparallel assemblies of the chains within the ribbon, as shown in Scheme 3.

($\Delta E = -0.3$ kcal mol^{-1}) with the H hydroxyl atom pointing toward the O atom of the bridge. Nevertheless, the trans conformation ($\tau = 180°$) appears to have the highest energy by ca. 4 kcal mol^{-1} with respect to the gauche ones. The carboxylic acid conformation does not affect qualitatively the stability of the conformations. The same conclusions hold for the (±)-**1f** model.

(b) Two-Dimensional Network. The crystal structure of (±)-**1d**,**i**,**g**,**q** is made up of layers. In (±)-**1q**, the layers consists of alternating chains (O4—H···O2 bonds) of enantiomers linked by O2—H···O3, giving rise to rings of different sizes (Figure 3a and Scheme 3).

In (±)-**1d** and **i**, the layered structures are formed by centrosymmetric dimers (through O2—H···O1 bonds) connected by O4H···O2 bonds (Figure 3b).

In (±)-**1g**, each independent molecule (Figure 3c) forms chains, and the packing arrangement of these chains resembles that of (±)-**1q**. If one chain is moved with respect to the contiguous one, this offset places the O2H in molecule A from the O2 and O3 in molecule B at 2.765(4) and 3.472(4) Å, respectively, leading to an $R_3^3(8)$ ring in this compound instead of $R_4^4(12)$ in (±)-**1q**, as illustrated in Figure 3a.

(c) Three-Dimensional Network. (±)-**1b**·$^1/_2H_2O$ crystallizes as a hemihydrate with a water and two independent molecules (A and B) in the asymmetric unit. Molecules B are arranged, through the water molecules (Ow—Hb···O3B and Ow—Ha···O2B) in chains around 2_1 axes, producing a $C_2^2(10)$ motif, marked with arrows in Figure 4a. These chains are then linked though the hydroxyl group of this molecule B [O4—H(mol. B)···O1(mol. B)], generating sheets. The hydroxyl groups of molecule A (O2—H···Ow, O4—H···O1) are involved in two hydrogen bonds along *b*, reinforcing the tubular structure, although there are not voids inside the $C_2^2(10)$ spirals. Molecules A and B are linked through an O4H···O bond.

In (+)-**1e**·H_2O, where only one enantiomer is present in the crystal structure, the molecules are connected only through water molecules to give a 3-D structure (Figure 4a).

As previously reported, in the 3-D structure of (±)-**1n**·H_2O,[8] the water molecules play an important role in holding the molecules together, forming an hexameric ring around the three-fold inversion center (Figure 4b) and connecting these rings along *c*, generating a tubular structure. This ring system is linked to another one by means of water molecules, which act as donors of two hydrogen bonds to O1 and O2 and acceptors of one strong hydrogen bond from O4. The rings stack in this way to give a porous channel, which holds disordered water molecules. The secondary structure of the anhydrous compound has been also included in Figure 4b for comparison. The ribbon is similar to that of (±)-**1f** (Figure 2a).

Discussion

Of the 16 compound studied, 13 generated crystal structures that do not present incorporation of water molecules. One of these anhydrous structures, the one corresponding to molecule

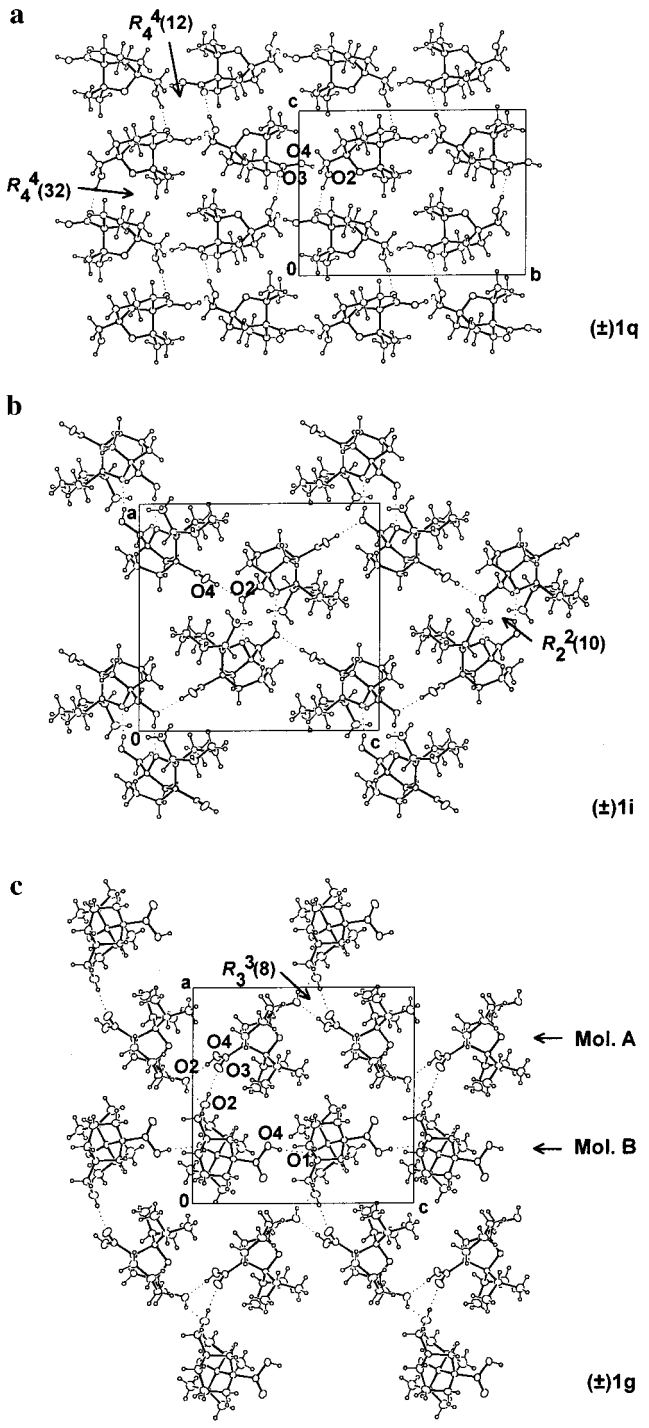

Figure 3. 2-D hydrogen bond network in (±)-**1q**, **i**, and **g**. Dotted lines represent O—H···O hydrogen interactions. The graph-set descriptors as well as labels of the oxygen atoms involved in the O—H···O hydrogen interactions have been included.

(±)-**1o**, gave a centrosymmetric dimer. It formed a discrete assembly about the inversion center that occurred by dimerization of both enantiomers. The remainder of the molecules that gave anhydrous crystals present translational symmetry in agreement with the predictions depicted in Scheme 3. Thus, the crystal structures of molecules (±)-**1a** and (±)-**1l** exhibit a 1-D network formed by dimerization of two parallel chains of enantiomers following the H-bonding pattern A. Six crystal structures involving molecules (±)-**1c**, **f**, **h**, **k**, **m**, and **p** exhibit antiparallel 1-D networks which can be associated with patterns B and B′. Four crystal structures corresponding to molecules (±)-**1d**, **g**, **i**, and **q** gave 2-D networks related to the assembly pattern defined as C in Scheme 3.

Three of the homologues studied, (±)-**1b**, **e**, and **n**, in the solid state gave 3-D networks by incorporation of molecules of water. Two of these hydrated structures, (±)-**1b**·$^1/_2H_2O$ and (+)-**1e**·H_2O, derived from interdigitated single-stranded chains composed of pure enantiomorphic molecules. Since hydroxy acid **1e** is racemic, enantiomeric separation of (+)-**1e**·H_2O takes place during crystallization with formation of a conglomerate. The hexameric structure of (±)-**1n**·H_2O corresponds to the cyclic aggregate of a hydrated head-to-tail single-stranded chain formed by alternating (+)- and (−)-**1n** molecules. These results show that the anhydrous assemblies depicted in Scheme 3 can be used as a platform with which to explain the 3-D molecular packing of hydrated crystals. Thus, depending on whether hydration occurred on a parallel (A′) or an antiparallel (B′) H-bonding pattern, we can expect hydrated head-to-tail single-stranded chains of alternating or pure enantiomorphic molecules, respectively. Only in the first case, disruption of the dimeric motif provides a single-stranded array in conditions favorable for ring packing, leading to the conclusion that the ethyl groups present in the racemic molecule **1n** define the optimized elements essential for the self-assembly described in Scheme 2.

An important feature of the crystalline structure of (±)-**1n**·H_2O is that the translationally related hexamers coincide with each other to describe channels that extend through the crystal. The key structural requirement for this motif was the spatial disposition of hydrogen bond donor and acceptor sites on both faces of the hexameric ring structure. [8] The molecules forming the hexameric unit are related by a three-fold inversion center, and the ethyl groups are oriented on the inner part of the ring, forming an irregular cylindrical hydrophobic surface of minimum and maximum diameter of 5.7 and 9.4 Å, respectively. It must be noted that ethyl groups are not specially involved in the construction of the hexameric aggregate; however, the ethyl groups pointing into the pore gave the correct volume to protect the structure from collapsing (Figure 5). This finding supports the idea that steric influences are the predominant factor involved in the closest packing and give an explanation for why all attempts to obtain, in the crystalline state, tubular structures by using homologues different from (±)-**1n** have failed. In many respects, the approach followed for the selection of the right homologue is analogous to the synthesis of biologically active molecules by modifying parts of the structure to fine-tune the precise properties of a drug. The basic concept is the same.

A major focus of this research is also to demonstrate, using sorption measurements, that the tubular structure shown by (±)-**1n**·H_2O can support permanent porosity and exhibit reversible inclusion properties that are uncommon to traditional organic porous materials. Table 4 compares the elemental microanalysis of the evacuated forms of the as-synthesized crystalline material prepared from racemic compounds **1n** and **1j**. The desolvated phase has been shown to have microporosity to N_2 sorption and will take up water when standing at room temperature. The ability of H_2O to reversibly pack the tubular structure would therefore appear to be critically important in sustaining the stability of the open 3-D polymeric network. All attempts to measure N_2 and Ar isotherms of the fully evacuated forms of these materials were unsuccessful, perhaps due to their inability to diffuse freely into the pores at low temperature.[28]

(28) These cases are in agreement with similar findings documented for zeolite sorption, which are attributed to possible obstructions within the channels that are amplified at lower temperatures: Breck, D. W. *Zeolite Molecular Sieves*; John Wiley & Sons: New York, 1974.

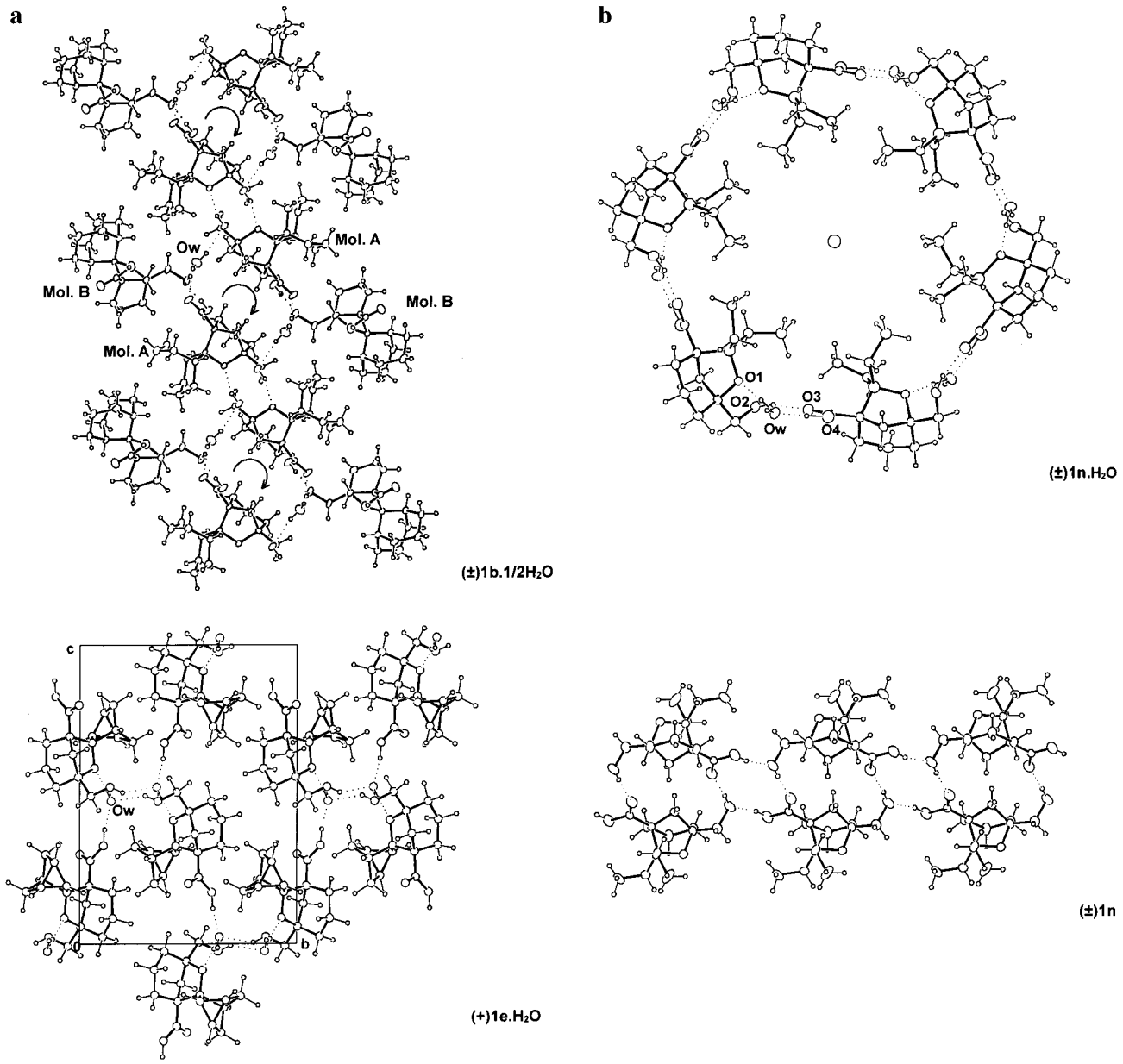

Figure 4. (a) Crystal packing of (±)-**1b**·$^1/_2H_2O$ and **1e**·H_2O. (b) Secondary structure of (±)-**1n**·H_2O showing the hexameric association and the same for (±)-**1n** displaying the 1-D network. Dotted lines represent O—H···O hydrogen interactions.

Single crystals of (±)-**1n**·H_2O were kept under vacuum (0.1 Torr) at 25 °C and then transferred to a glovebox under dry Ar to give, after crystallization from dry benzene, anhydrous crystals. The crystal structure of (±)-**1n** packed in a 1-D network formed by dimerization of two antiparallel chains of enantiomers following the H-bonding pattern B (Scheme 3). This result further shows the necessity of water molecules in the reversion from linear to hexagonal orders, according to the predictions depicted in the retrosynthetic analysis (Scheme 2). Furthermore, pure (−)-**1n** enantiomer [29] results in be an oily, noncrystalline substance, which demonstrates the importance of both enantiomers in the formation of the crystalline state.

The bulk structure of organic crystals can often be described as layers that stack in the remaining third dimension. The crystalline structures reported here show that layers pucker to different extents, reflexting an intrinsic flexibility that enables both linear (anhydrous) and cyclic (hydrated) motifs to exist initially in equilibrium, despite the differently sized groups included within the networks. Nevertheless, the closest packing of hexagonal pores in adjacent sheets to give tubular structures apparently is quite sensitive to steric interactions, given that linear anhydrous networks were most commonly observed. The demonstrated stability of hydrated cyclic aggregates in the optimized homologue **1n** suggests that such a supramolecular structure might also reasonably be found in a lipid membrane environment.[30] We have reported[8] the ability of many of these racemic compounds, i.e., **1a**, **1b**, **1j**, and **1n**, to facilitate transmembrane sodium transport in phosphatidylcholine bilayers. In this context, our next step is to determine if lipophilic hexameric aggregates function as ion channels in lipid membranes.[31]

(29) The enantiomer (−)-**1n**, [α] = − 28.0° ($CHCl_3$, c = 1.2), was obtained from the racemic mixture by resolution involving recrystallization of the salt with L-(−)-α-methylbenzylamine from acetone. The acid (−)-**1n** was recovered from the salt by treatment with 6 N hydrochloric acid and ether, washing with a small amount of saturated Na_2SO_4, and evaporation of ether.

(30) For an excellent recent review related to organic tubular structures, see: Bong, D. T.; Clark, T. D.; Granja, J. R.; Ghadiri, M. R. *Angew. Chem., Int. Ed.* **2001**, *40*, 988.

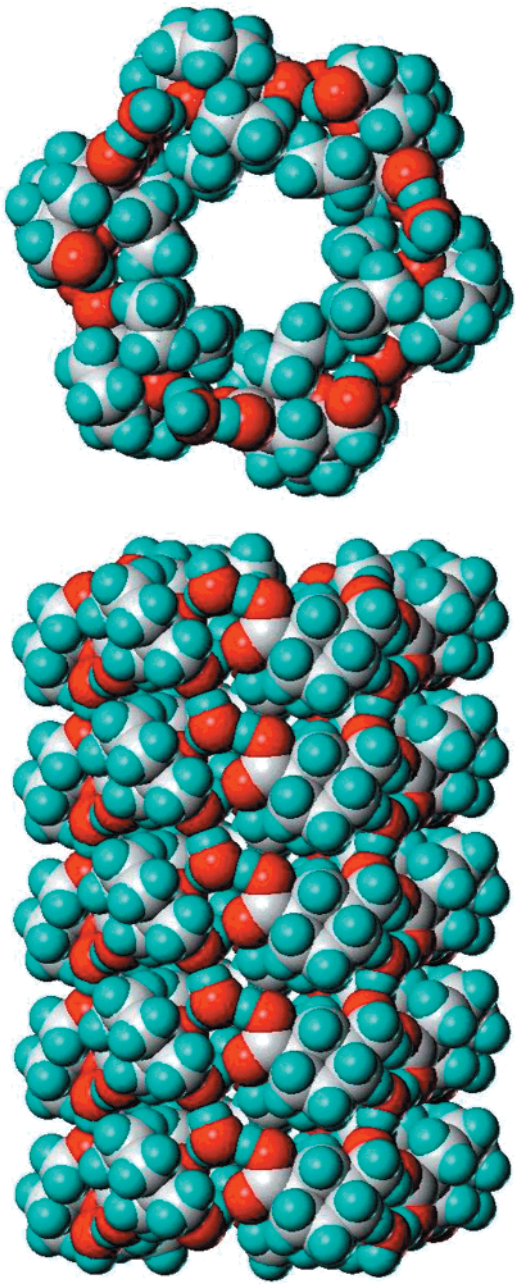

Figure 5. Front and side space-filling projections of the crystal structure of (±)-**1n**·H_2O showing the open pore and the hexameric chairlike aggregation. White, red, and blue circles represent carbon, oxygen, and hydrogen atoms, respectively.

Conclusions

Although a few natural[32] and synthetic[13,14] compounds were shown to form supermacrocyclic assemblies in solution, and in solid and liquid crystalline states, none are known to form macrocycles or discrete tubular assemblies by incorporation of water molecules into their structures. We anticipate in this work that the equilibrium between anhydrous (linear) and hydrated (cyclic) forms can be optimized to give an isostructural porous 3-D network in crystalline solids. The results achieved here demonstrate that it is the combined steric requirements and the conformational flexibility that govern which framework is adapted and argue that the architecture of these materials can be rationally manipulated by systematic, stepwise changes in the size of the monomers. Additionally, these results illustrate that the crystal structure is simplified when structurally robust supramolecular synthons are employed. In this case, the reliability of the axially oriented hydroxyl/carboxylic acid functions to give anhydrous layers reduces the design of the last remaining dimension to the reversible incorporation of water molecules. This last motive can also be rationalized by following carefully designed retrosynthetic approaches.

Table 4. Calculated and Found (Shown in *Italics*) Elemental Composition of Compounds (±)-**1n** and (±)-**1j**: (A) As-Synthesized), (B) Evacuated, and (C) Evacuated after 15 Days in Contact with Air

	(±)-**1n**				(±)-**1j**			
	C	H	N	O	C	H	N	O
A	$C_{13}H_{22}O_4 \cdot H_2O$				$C_{15}H_{26}O_4 \cdot H_2O$			
	59.98	9.29		30.73	62.47	9.97		27.74
	59.92	*9.67*	*0.25*	*30.16*	*62.41*	*9.41*	*0.18*	*28.00*
B	$C_{13}H_{22}O_4$				$C_{15}H_{26}O_4$			
	64.44	9.15		26.41	66.64	9.69		23.67
	64.20	*9.28*	*2.25*	*24.27*	*66.65*	*9.80*	*1.89*	*21.66*
C	$C_{13}H_{22}O_4 \cdot H_2O$				$C_{15}H_{26}O_4 \cdot H_2O$			
	59.98	9.29		30.73	62.47	9.79		27.74
	60.27	*9.31*	*0.51*	*29.91*	*62.61*	*9.27*	*0.37*	*27.75*

Experimental Section

Compounds (±)-**1a**−(±)-**1q** were synthesized by following a previously reported methodology.[33] The general experimental procedures were recently described elsewhere.[34] Full characterization data are presented in the Supporting Information.

Crystals of all compounds were grown under identical conditions using a previously water-saturated mixture of carbon tetrachloride/*n*-hexane as solvent. Crystal data and experimental details are summarized in Table 5 (Supporting Information). The structures were solved by direct methods (Sir97[35] and SHELXS97[36]) and refined by least-squares on F^2. In most compounds, all hydrogen atoms were located on the corresponding difference synthesis and, when possible, refined isotropically; otherwise, idealized OH positions were computed so that the C−C−O−H torsion angle maximizes the electron density.

In (±)-**1k** and **h**, the hydrogens of the hydroxyl and carboxylic groups appear to be disordered (with the following occupancy factors: (±)-**1k**, pp(H4a,H2a) = 0.62(6), pp(H4b,H2a) = 0.38(6); (±)-**1h**, pp = 0.50]. The low precision reached in (±)-**1a** is mainly due to the twinned crystal used in data collection. Several crystals were checked in order to find a single crystal, and the one with the lowest spread was used for data collection. Most of the calculations were performed using the SHELXL97[37] and XTAL3.6[38] system of programs. (±)-**1a**, **c**, **d**, **e**, **k**, **n**, **o**, and **p** were collected on a Nonius CAD4 four-circle diffractometer, fine-focus, sealed tube, graphite monochromator, MoKα radiation (λ = 0.0707 Å), and ω scans, while data for compounds (±)-**1b**, **f**, **g**, **h**, **i**, **l**, and **m** were recorded using a CCD area detector, Brucker

(31) Most importantly, enantiomer (−)-**1n** is inactive at any concentration, indicating that both enantiomers are necessary to foster cation flux in membranes.

(32) (a) Marsh, T. C.; Vesenka, J.; Henderson, E. *Nucleic Acids. Res.* **1995**, *23*, 696. (b) Gottarelli, G.; Mezzina, E.; Spada, G. P.; Carsughi, F.; DiNicola, G.; Mariani, P.; Sabaticci, A.; Bonazzi, S. *Helv. Chim. Acta* **1996**, *79*, 220. (c) Forman, S. L.; Fettinger, J. C.; Pieraccini, S.; Gotarelli, G.; Davis, J. T. *J. Am. Chem. Soc.* **2000**, *122*, 4060.

(33) Martín, J. D.; Pérez, C.; Ravelo, J. L. *J. Am. Chem. Soc.* **1986**, *108*, 7801.

(34) Brouard, I.; Hanxing, L.; Martín, J. D. *Synthesis* **2000**, 883.

(35) Altomare, A.; Cascarano, G.; Giacovazzo, C.; Guagliardi, A.; Moliterni, A. G. G.; Burla, M. C.; Polidori, G.; Camalli, M.; Spagna, R. SIR97. *A Package for Crystal Structure Solution by Direct methods and Refinement;* University of Bari, Italy, 1997.

(36) Sheldrick, G. M. *Acta Crystallogr*. **1990**, *A46*, 467.

(37) Sheldrick, G. M., SHELXL97, Univerity of Gottingen, Germany.

(38) Hall, S. R.; du Boulay, D. J.; Olthof-Hazekamp, R., Eds. *The Xtal System of Crystallographic Software. "XTAL3. 6" User's Manual*; The University of Western Australia, Australia, 1999.

SMART fine-focus, sealed tube, graphite monochromator, MoKα radiation ($\lambda = 0.0707$Å), $\omega/2\theta$ and ω scans.

In (+)-**1e**, a new data set using CuKα radiation did not permit the determination of the absolute configuration since the refinement of the Flack parameter[39] led to unreliable values due to the lack of sufficient anomalous scatters. The reported geometrical parameters correspond to the Mo dataset.

Acknowledgment. We thank Miguel Ángel Maestro and José Mahía (Servicios Xerais de Apoio á Investigación, Universidade da Coruña, Spain) for crystallographic services and many useful comments about the X-ray diffraction results. This work was financially supported by the Spanish DGICYT (Grants BQU2001-1137 and BQU2000-0868) and Gobierno de Canarias (Grants PI2001/038 to M.L.R. and CEE-FEDER (1FD97-0474-C04-01)). H.C. thanks the AECI, Spain, for a Predoctoral Fellowship.

(39) Flack, H. D. *Acta Crystallogr.* **1983**, *A39*, 876.

Supporting Information Available: Complete characterization data for compounds (±)-**1a**−(±)-**1q** (PDF). Tables of X-ray crystallographic data for compounds (±)-**1a**−(±)-**1d**, **1e**, (±)-**1f**−(±)-**1i**, and (±)-**1k**−(±)-**1p** (CIF). This material is available free of charge via the Internet at http://pubs.acs.org.

JA011028T